Applied Physics Letters

Detecting the out-of-time-order correlations of dynamical quantum phase transitions in a solid-state quantum simulator

Cite as: Appl. Phys. Lett. **116**, 194002 (2020); https://doi.org/10.1063/5.0004152
Submitted: 08 February 2020 . Accepted: 30 April 2020 . Published Online: 11 May 2020

Bing Chen, Xianfei Hou, Feifei Zhou, Peng Qian, Heng Shen, and Nanyang Xu

Applied Physics Letters ARTICLE scitation.org/journal/apl

Detecting the out-of-time-order correlations of dynamical quantum phase transitions in a solid-state quantum simulator

Cite as: Appl. Phys. Lett. **116**, 194002 (2020); doi: 10.1063/5.0004152
Submitted: 8 February 2020 · Accepted: 30 April 2020 ·
Published Online: 11 May 2020

Bing Chen,[1,2] Xianfei Hou,[1] Feifei Zhou,[1] Peng Qian,[1] Heng Shen,[3,a)] and Nanyang Xu[1,b)]

AFFILIATIONS

[1]School of Electronic Science and Applied Physics, Hefei University of Technology, Hefei, Anhui 230009, China
[2]State Key Laboratory of Quantum Optics and Quantum Optics Devices, Shanxi University, Taiyuan 030006, China
[3]Clarendon Laboratory, University of Oxford, Parks Road, Oxford OX1 3PU, United Kingdom

[a)]Author to whom correspondence should be addressed: heng.shen@physics.ox.ac.uk
[b)]Electronic mail: nyxu@hfut.edu.cn

ABSTRACT

Quantum many-body systems in equilibrium can be effectively characterized using the framework of quantum statistical mechanics. However, there still exist a lot of questions regarding how to understand the nonequilibrium dynamical behavior of quantum many-body systems, which are not accessible with the thermodynamic description. Experiments in quantum simulators are opening up a route toward the generation of quantum states beyond the equilibrium paradigm. As an example, in closed quantum many-body systems, dynamical quantum phase transitions act as phase transitions in time, with physical quantities becoming nonanalytic at a critical time, extending important principles such as universality to the nonequilibrium realm. Here, in a solid-state quantum simulator, we report the experimental detection of out-of-time-order correlators in the presence of nonequilibrium phase transitions with the transverse field Ising model, which are a central concept to quantify quantum information scrambling and quantum chaos. Through measuring the multiple quantum spectra, we eventually observe the buildup of quantum correlation. Further applications of this protocol could potentially enable studies of other exotic phenomena such as many-body localization and tests of the holographic duality between quantum and gravitational systems.

Equilibrium properties of quantum matter can be effectively captured with the well-established quantum statistical mechanics. However, when closed quantum many-body systems are driven out of equilibrium, a lot of questions about how to understand the actual dynamics of quantum phase transitions remain elusive since they are not accessible with the thermodynamic description.[1,2] An exciting perspective arises from quantum simulators, which can mimic natural interacting quantum many-body systems with experimentally controlled quantum matter such as ultracold atoms in optical lattices and trapped ions. Such analog systems enable the investigation of exotic phenomena such as many-body localization,[3,4] prethermalization,[5,6] particle–antiparticle production in the lattice Schwinger model,[7] dynamical quantum phase transitions (DQPTs),[8–15] and discrete time crystals.[16,17]

In many of these phenomena, such as the celebrated logarithmic entanglement growth in many-body localization,[18–20] the propagation of quantum information plays a central role, opening up a point of view and possibilities for probing out-of-equilibrium dynamics. To measure the propagation of information beyond quantum correlation spreading and characterize quantum scrambling through quantum many-body systems, the concept of out-of-time-order correlation (OTOC) has been developed recently,[21–26] providing insight into quantum chaos[27,28] and black hole information problems.[29,30]

Recent experimental progress in measuring out-of-time-order correlation (OTOC)[23–25,31] delivers important insight into a more thorough grasping of how such quantities characterized complex quantum systems. For instance, OTOC can be used as entanglement witness via multiple quantum coherence[32] and, in particular, be used to dynamically detect equilibrium as well as nonequilibrium phase transitions.[33,34] Here, we emulate the dynamical quantum phase transitions of quantum many-body systems with the transverse field Ising (TFI) model by a solid-state quantum simulator based on the nitrogen-vacancy (NV) center in diamond.[35] Furthermore, the measurement of OTOC is performed to quantify the buildup of quantum

correlations and coherence, and remarkably, the results exhibit specific features in the occurrence of dynamical phase transitions.

A very general setting for DQPT is the one emerging from a sudden global quench across an equilibrium quantum critical point,[8,9,36] and DQPT manifests itself in discontinuous behavior of the system at certain critical times. Here, we consider such a protocol. First, the state is initialized in the ground state of the initial Hamiltonian $\hat{H}_0 = -\sum_i^N \hat{\sigma}_i^x \hat{\sigma}_{i+1}^x$ as $|\Phi\rangle_0 = |+\rangle^{\otimes N}$, where $|+\rangle = (|\uparrow\rangle + |\downarrow\rangle)/\sqrt{2}$ and N is the number of spins. At time t = 0, the Hamiltonian is suddenly switched to $\hat{H}_{TFI} = -\sum_i^N (\hat{\sigma}_i^x \hat{\sigma}_{i+1}^x + g\hat{\sigma}_i^z)$ and the system state evolves to $|\Phi(t)\rangle = e^{-i\hat{H}t}|\Phi\rangle_0$, realizing a quantum quench. Here, $\hat{\sigma} = (\hat{\sigma}^x, \hat{\sigma}^y, \hat{\sigma}^z)$ are Pauli spin operators. The rate function $f(t)$ as a function of return probability plays a role of a dynamical free energy, signaling the occurrence of DQPT.

Strikingly, a variety of many-body systems with a large number of spin-1/2 states can be studied in momentum space by a two-band model with decoupled momentum modes (thus can be simulated independently), which is equivalent to a single spin-1/2 state evolving on the Bloch sphere for each mode (so-called relative Bloch sphere, see Ref. 37). To explore DQPT of a spin-chain via a single solid-state qubit, $\hat{H}_{TFI}$ is written in momentum space as $\hat{H}_{TFI} = \sum_k \Psi_k^\dagger \hat{H}_k \Psi_k$, where Ψ_k denotes a spinor with a two element vector composed of fermion operators (see the supplementary material). The associated Bloch Hamiltonian is $\hat{H}_k = \mathbf{d}(k) \cdot \hat{\sigma} = [1 - \cos(k)g]\hat{\sigma}_x + \sin(k)g\hat{\sigma}_y$, with k being the quasi-momentum. The bulk dynamics of the system can be solved since each k-component evolves independently, and the state at each k is given by $|\Phi(k,t)\rangle = e^{-i\hat{H}_k t}|\Phi(k,0)\rangle$ after quantum quench control. The rate function is defined as $f(t) = -1/N \sum_k \log(\langle\Phi(k,0)|e^{-i\hat{H}_k t}|\Phi(k,0)\rangle)^2$, whose nonanalytic behavior yields DQPT.

In the experiment, we use a negatively charged NV center in a type-IIa, single-crystal synthetic diamond sample (Element Six) to simulate the quantum many-body dynamics in its quasi-momentum representation. Purpose-built scanning confocal microscopy is employed to address the single NV center and detect the fluorescence photons, as shown in Fig. 1(a). As illustrated in Fig. 1(b), both the ground state ($^3A_2$) and the excited state (^3E) of the NV center are spin triplet states,[38,39] and the transition between the two states corresponds to the zero-phonon line (ZPL) at 637 nm (1.945 eV). We encode $m_s = -1$ and $m_s = 0$ in $^3A_2$ as spin up and down of the electron spin qubit. The state of the qubit can be manipulated with microwave pulses ($\omega_{MW} \approx 2\pi \times$ 1400 MHz), while the spin level $m_s = +1$ remains idle due to large detuning. By applying a laser pulse of 532 nm wavelength with the assistance of intersystem crossing (ISC) transitions,[40] the spin state can be polarized into $m_s = 0$ in the ground state.[41] This process can be utilized to initialize and read out the spin state of the NV center. The fluorescence photons are detected by using the single photon counting module (SPCM). By using a permanent magnet, a magnetic field about 524 G is applied along the NV axis, and the ^{14}N nuclear spin associated with the NV center is polarized with optical pumping, which is enabled by the level anti-crossing in its excited state.[42] Nuclear spin polarization can improve the coherence time of the electron spin. It is observed in the optically detected magnetic resonance (ODMR) spectra that the nuclear spin polarization is higher than 98%.

Experimentally, for each decoupled momentum mode in the first Brillouin zone, evolution at different k values is performed in

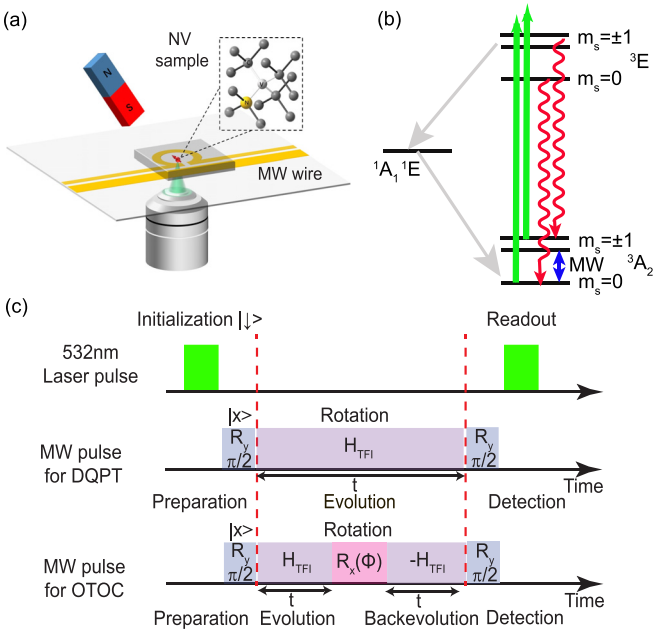

FIG. 1. Measuring out-of-time-order correlation using time reversal in the NV center. (a) Illustration of experimental schematics and the atomic structure of the NV center in diamond. (b) Scheme of energy levels of the NV center electron spin. (c) Laser and microwave pulse sequence for the measurement of DQPT and OTOC. The $\pi/2$ rotation $\hat{R}_y$ about the y-axis prepares an initial state with spin pointing along the x-axis $|x\rangle$. The state of interest $\hat{\rho}(t)$ is reached after the first evolution period. The rotation $\hat{H}_{TFI}$ is the quantum quench control. The phase of $\hat{H}_{TFI}$ is different for each momentum mode k. The rotation $\hat{R}_x(\phi)$ then imprints a phase $m\phi$ on each sector $\hat{\rho}_m$ of the density matrix. Evolving backward and measuring the overlap with the initial state as a function of ϕ, the coherence I_m and magnetization A_m of $\hat{\rho}(t)$ are retrieved as the Fourier components of this signal.

independent runs attributed to different rotation axes and speeds (see the supplementary material). As sketched in Fig. 1(c), we start the sequence with 1μs laser pulses to polarize the NV center electron spin and nearby nuclear spins into state $|\downarrow\rangle$. Then, the qubit is prepared into the ground state of $\hat{H}_0$ as $|+\rangle = (|\uparrow\rangle + |\downarrow\rangle)/\sqrt{2}$ by a $\pi/2$ microwave pulse. After that, we switch on the second microwave pulse for the quantum quench rotation operation $\hat{H}_{TFI}$. The return probabilities are recorded by projecting the final states on the x-basis by another $\pi/2$ microwave pulse. These microwave pulses for spin operations are generated from an in-phase (I) and quadrature-phase (Q) modulation system where we use an arbitrary waveform generator (Tektronix AWG510) to synthesize different durations and phases. In the transverse field Ising model, the critical transverse field $g_c = 1$ separates the paramagnetic phase ($g > 1$) from the ferromagnetic phase ($g < 1$). Since the state is initialized in the ferromagnetic phase ($g_i = 0$), DQPT can occur only if $g_f > 1$. It is demonstrated by the experimental data of the rate function for different g_f values, as shown in Fig. 2(a), where the sharp peak with nonanalytic behavior of the rate function indicates the DQPT, being associated with dynamical Fisher zeros[43] (see the supplementary material).

fFurther signatures of the DQPT are observed by measuring the OTOC, a quantity probing the spread of quantum information beyond quantum correlations. OTOC functions of particular interest are defined

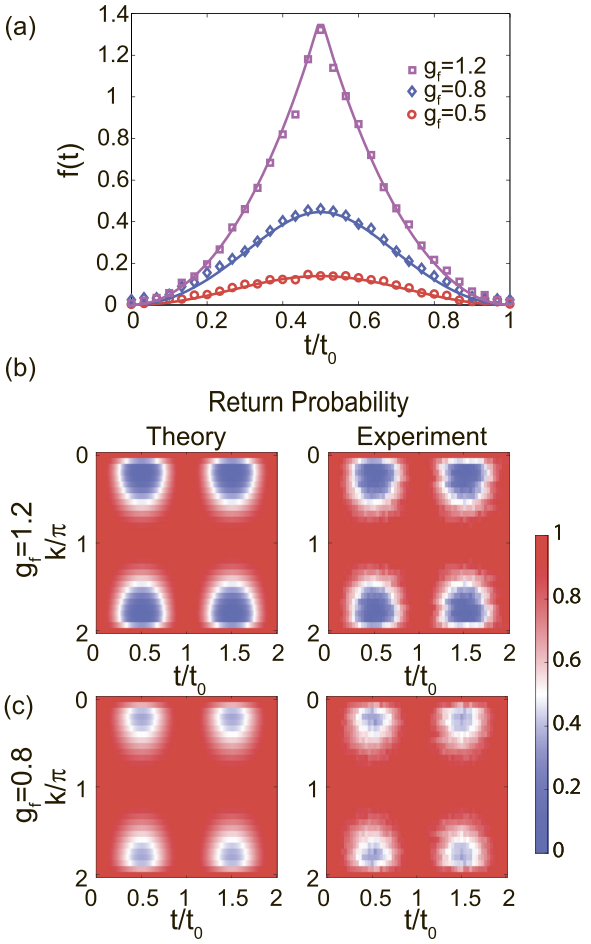

FIG. 2. Rate function and return probabilities after a quantum quench in an Ising model. (a) Rate function after a quantum quench of $\hat{H}_{TFI} = -\sum_i^N (\hat{\sigma}_i^x \hat{\sigma}_{i+1}^x + g_f \hat{\sigma}_i^z)$, with N = 30. The initial state is prepared at $|\phi_i\rangle = |\underrightarrow{x}\rangle = (|\uparrow\rangle + |\downarrow\rangle)/\sqrt{2}$, as the ground state of $\hat{H}_0 = -\sum_i^N \hat{\sigma}_i^x \hat{\sigma}_{i+1}^x$ (i.e., $g_i = 0$ in $\hat{H}_{TFI}$). g_f is varied in the global quench with the values of 0.5, 0.8, and 1.2. Rate functions are shown in panel (a), with symbols (red circle, blue diamond, and magenta square) and solid lines representing experimental data and theoretical values. We theoretically calculate the spin state evolution experiencing a series of unitary operations and obtain the theory curve. [(b) and (c)] Return probabilities for $g_f = 1.2$ and $g_f = 0.8$, respectively. Theoretical results and experimental data are presented in the left and right panels, all sharing the same colorbar. For convince, t is normalized by a period of time $t_0 = \pi/|\mathbf{d}_f(k)|$ (see the supplementary material).

as, Refs. 23 and 44, $F(t) = \langle \hat{W}^\dagger(t)\hat{V}^\dagger \hat{W}(t)\hat{V}\rangle$, where $\hat{W}(t) = e^{i\hat{H}_{int}t}\hat{W}e^{-i\hat{H}_{int}t}$, with $\hat{H}_{int}$ being an interacting many-body Hamiltonian and $\hat{W}$ and $\hat{V}$ two commuting unitary operators. $\mathrm{Re}[F(t)] = 1 - \langle|[\hat{W}(t), \hat{V}]|^2\rangle/2$ captures the degree by which the initially commuting operators fail to commute at later times due to the many-body interactions $\hat{H}_{int}$, an operational definition of the scrambling rate. In such a process, the information initially encoded in the state spread over the other degrees of freedom of the system after the interactions and cannot be retrieved by local operations and measurements.

We now outline the protocol to measure the OTOC as illustrated in Fig. 1(c). In contrast to the pulse sequence for DQPT, we implement the many-body time reversal by inverting the sign of $\hat{H}_{TFI}$, which evolves again for time t to the final state ρ_f and ideally takes the system back to the initial state ρ_0. If a state rotation $\hat{R}_x(\phi) = e^{-i\hat{S}_x\phi}$, i.e., $\hat{W}(0) = \hat{R}_x(\phi)$, here about the x-axis with $\hat{S}_x = 1/2\sum_i \hat{\sigma}_x^i$, is inserted between the two halves of the time evolution through a variable angle ϕ, the dependence of the revival probability on this angle contains information about $\rho(t)$. At the end of the sequence, two different observables can be measured, the collective magnetization along the x-direction $\langle \hat{S}_x\rangle = tr[\hat{S}_x\hat{\rho}_f]$ and the fidelity $\mathscr{F}_\phi(t) = tr[\hat{\rho}_0\hat{\rho}_f]$. In particular, the fidelity can be cast as an OTOC by setting $\hat{V} = \hat{\rho}_0$, corresponding to a many-body Loschmidt echo. The measurement of the fidelity is also directly linked to the so-called multiple quantum intensities I_m by the Fourier transformation $\mathscr{F}_\phi(t) = tr[\hat{\rho}_f\hat{\rho}_0] = tr[\hat{\rho}(t)\hat{\rho}_\phi(t)] = \sum_{m=-N}^{N} I_m(t)e^{im\phi}$.[23,32,45] Similarly, the dynamics of the Fourier amplitude A_m of the magnetization $F_\phi(t) = \sum_{m=-N}^{N} A_m(t)e^{im\phi}$ quantifies the buildup of many-body correlations. However, it is much less sensitive to decoherence compared to the fidelity due to the nature of single-body observables.

In Fig. 3, we show the results of the magnetization OTOC measurement sequence and hence a buildup of Fourier amplitudes A_m, which are in good agreement with theoretical calculations. Comparison of the data with $g_f = 0.8$ to those with $g_f = 1.2$ confirms that the appearance of double-well-like features in the $\phi - t$ plane signals the DQPT. Figure 3(c) shows the measured magnetization with fixed $\phi = \pi$ by varying g_f, in agreement with the numerical simulation. The associated Fourier amplitude A_m is extracted and illustrated in Figs. 3(d) and 3(e). It is observed that the double-well feature distinguishes the DQPT with non-DQPT.

In summary, we demonstrate an approach for investigating quantum many-body system out of equilibrium by a solid-state quantum simulator based on the NV center in diamond. The sharp peak with nonanalytical behavior of the rate function indicates the DQPT.

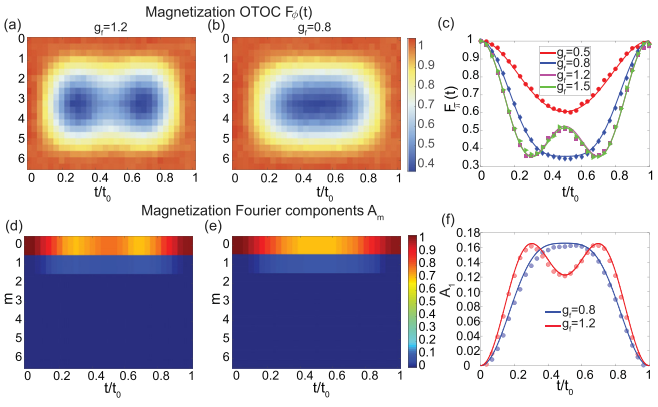

FIG. 3. Probing the DQPT through magnetization OTOC dynamics. The measured magnetization OTOC from time evolution under $\hat{H}_{TFI}$ and rotations about the x-axis $0 - 2\pi$ with $g_f = 1.2$ (a) and $g_f = 0.8$ (b). The associated Fourier component A_m dynamics for $g_f = 1.2$ (d) and $g_f = 0.8$ (e). (c) The measured magnetization with fixed $\phi = \pi$ by varying g_f (0.5, 0.8, 1.2, 1.5). (f) Fourier components A_1 as a function of time where the inversed double-well structure at the critical time t_c is only shown in DQPT ($g_f > 1$). In panels (c) and (f), these symbols and solid lines represent the experimental data and numerical simulations, respectively. The numerical simulations are developed by calculating the spin state evolution experiencing a series of unitary operations with the model in the supplementary material.

Moreover, we measure the magnetization OTOC to quantify the buildup of quantum correlations and coherence, and, in particular, the intriguing feature arising from the dynamical phase transitions is observed in the occurrence of DQPT. Further applications of this protocol could enable studies of other exotic phenomena such as many-body localization.

See the supplementary material for the theory of spin-chain model and the detailed experimental setup.

The authors are grateful to Philipp Hauke, Markus Heyl, and Xiaojun Jia for fruitful discussions. This work was supported by the National Key R&D Program of China (Grant Nos. 2018YFA0306600 and 2018YFF01012500), the National Natural Science Foundation of China (Grant Nos. 11604069 and 11904070), the Program of State Key Laboratory of Quantum Optics and Quantum Optics Devices (Grant No. KF201802), and the Fundamental Research Funds for the Central Universities (No. PA2019GDQT0023). H. Shen acknowledges the financial support from the Royal Society Newton International Fellowship (No. NF170876) of UK.

REFERENCES

[1]J. Eisert, M. Friesdorf, and C. Gogolin, Nat. Phys. **11**, 124–130 (2015).
[2]T. Langen, R. Geiger, and J. Schmiedmayer, Annu. Rev. Condens. Matter Phys. **6**, 201 (2015).
[3]M. Schreiber, S. S. Hodgman, P. Bordia, H. P. Lüschen, M. H. Fischer, R. Vosk, E. Altman, U. Schneider, and I. Bloch, Science **349**, 842–845 (2015).
[4]J. Smith, A. Lee, P. Richerme, B. Neyenhuis, P. W. Hess, P. Hauke, M. Heyl, D. A. Huse, and C. Monroe, Nat. Phys. **12**, 907–911 (2016).
[5]M. Gring, M. Kuhnert, T. Langen, T. Kitagawa, B. Rauer, M. Schreitl, I. Mazets, D. Adu Smith, E. Demler, and J. Schmiedmayer, Science **337**, 1318–1322 (2012).
[6]B. Neyenhuis, J. Zhang, P. W. Hess, J. Smith, A. C. Lee, P. Richerme, Z.-X. Gong, A. V. Gorshkov, and C. Monroe, Sci. Adv. **3**, e1700672 (2017).
[7]E. A. Martinez, C. A. Muschik, P. Schindler, D. Nigg, A. Erhard, M. Heyl, P. Hauke, M. Dalmonte, T. Monz, P. Zoller, and R. Blatt, Nature **534**, 516–519 (2016).
[8]P. Jurcevic, H. Shen, P. Hauke, C. Maier, T. Brydges, C. Hempel, B. P. Lanyon, M. Heyl, R. Blatt, and C. F. Roos, Phys. Rev. Lett. **119**, 080501 (2017).
[9]J. Zhang, G. Pagano, P. W. Hess, A. Kyprianidis, P. Becker, H. Kaplan, A. V. Gorshkov, Z.-X. Gong, and C. Monroe, Nature **551**, 601–604 (2017).
[10]N. Fläschner, D. Vogel, M. Tarnowski, B. S. Rem, D.-S. Lühmann, M. Heyl, J. C. Budich, L. Mathey, K. Sengstock, and C. Weitenberg, Nat. Phys. **14**, 265–268 (2018).
[11]K. Yang, L. Zhou, W. Ma, X. Kong, P. Wang, X. Qin, X. Rong, Y. Wang, F. Shi, J. Gong, and J. Du, Phys. Rev. B **100**, 085308 (2019).
[12]X.-Y. Guo, C. Yang, Y. Zeng, Y. Peng, H.-K. Li, H. Deng, Y.-R. Jin, S. Chen, D. Zheng, and H. Fan, Phys. Rev. Appl. **11**, 044080 (2019).
[13]H. Lang, Y. Chen, Q. Hong, and H. Fan, Phys. Rev. B **98**, 134310 (2018).
[14]J. C. Halimeh and V. Zauner-Stauber, Phys. Rev. B **96**, 134427 (2017).
[15]J. Lang, B. Frank, and J. C. Halimeh, Phys. Rev. Lett. **121**, 130603 (2018).
[16]J. Zhang, P. W. Hess, A. Kyprianidis, P. Becker, A. Lee, J. Smith, G. Pagano, I.-D. Potirniche, A. C. Potter, A. Vishwanath, N. Y. Yao, and C. Monroe, Nature **543**, 217–220 (2017).
[17]S. Choi, J. Choi, R. Landig, G. Kucsko, H. Zhou, J. Isoya, F. Jelezko, S. Onoda, H. Sumiya, V. Khemani *et al.*, Nature **543**, 221–225 (2017).
[18]M. Žnidarič, T. Prosen, and P. Prelovšek, Phys. Rev. B **77**, 064426 (2008).
[19]J. H. Bardarson, F. Pollmann, and J. E. Moore, Phys. Rev. Lett. **109**, 017202 (2012).
[20]E. Altman, Nat. Phys. **14**, 979–983 (2018).
[21]B. Swingle, Nat. Phys. **14**, 988–990 (2018).
[22]R. J. Lewis-Swan, A. Safavi-Naini, A. M. Kaufman, and A. M. Rey, Nat. Rev. Phys. **1**, 627–634 (2019).
[23]M. Gärttner, J. G. Bohnet, A. Safavi-Naini, M. L. Wall, J. J. Bollinger, and A. M. Rey, Nat. Phys. **13**, 781–786 (2017).
[24]J. Li, R. Fan, H. Wang, B. Ye, B. Zeng, H. Zhai, X. Peng, and J. Du, Phys. Rev. X **7**, 031011 (2017).
[25]K. A. Landsman, C. Figgatt, T. Schuster, N. M. Linke, B. Yoshida, N. Y. Yao, and C. Monroe, Nature **567**, 61–65 (2019).
[26]C. M. Sánchez, A. K. Chattah, K. X. Wei, L. Buljubasich, P. Cappellaro, and H. M. Pastawski, Phys. Rev. Lett. **124**, 030601 (2020).
[27]J. Maldacena, S. H. Shenker, and D. Stanford, J. High Energy Phys. **2016**, 106.
[28]P. Hosur, X.-L. Qi, D. A. Roberts, and B. Yoshida, J. High Energy Phys. **2016**, 4.
[29]P. Hayden and J. Preskill, J. High Energy Phys. **2007**, 120.
[30]S. H. Shenker and D. Stanford, J. High Energy Phys. **2014**, 67.
[31]M. K. Joshi, A. Elben, B. Vermersch, T. Brydges, C. Maier, P. Zoller, R. Blatt, and C. F. Roos, arXiv:2001.02176 (2020).
[32]M. Gärttner, P. Hauke, and A. M. Rey, Phys. Rev. Lett. **120**, 040402 (2018).
[33]M. Heyl, F. Pollmann, and B. Dóra, Phys. Rev. Lett. **121**, 016801 (2018).
[34]C. B. Dağ, K. Sun, and L.-M. Duan, Phys. Rev. Lett. **123**, 140602 (2019).
[35]B. Chen, J. Geng, F. Zhou, L. Song, H. Shen, and N. Xu, Appl. Phys. Lett. **114**, 041102 (2019).
[36]M. Heyl, Rep. Prog. Phys. **81**, 054001 (2018).
[37]J. C. Budich and M. Heyl, Phys. Rev. B **93**, 085416 (2016).
[38]M. W. Dohertya, N. B. Mansonb, P. Delaneyc, F. Jelezkod, J. Wrachtrupe, and L. C. L. Hollenberg, Phys. Rep. **528**, 1–45 (2013).
[39]J. Harrison, M. J. Sellars, and N. B. Manson, J. Lumin. **107**, 245–248 (2004).
[40]M. L. Goldman, A. Sipahigil, M. W. Doherty, N. Y. Yao, S. D. Bennett, M. Markham, D. J. Twitchen, N. B. Manson, A. Kubanek, and M. D. Lukin, Phys. Rev. Lett. **114**, 145502 (2015).
[41]L. Robledo, H. Bernien, T. V. Der Sar, and R. Hanson, New J. Phys. **13**, 025013 (2011).
[42]V. Jacques, P. Neumann, J. Beck, M. Markham, D. Twitchen, J. Meijer, F. Kaiser, G. Balasubramanian, F. Jelezko, and J. Wrachtrup, Phys. Rev. Lett. **102**, 057403 (2009).
[43]S. Vajna and B. Dóra, Phys. Rev. B **91**, 155127 (2015).
[44]A. I. Larkin and Y. N. Ovchinnikov, ZhETF **55**, 2262 (1968) [Sov. Phys. JETP **28**, 1200 (1969)].
[45]N. Y. Yao, F. Grusdt, B. Swingle, M. D. Lukin, D. M. Stamper-Kurn, J. E. Moore, and E. Demler, arXiv:1607.01801 (2016).